



## Formation of the April 2007 caldera collapse at Piton de La Fournaise volcano: Insights from GPS data

Aline Peltier <sup>a,b,\*</sup>, Thomas Staudacher <sup>b</sup>, Patrick Bachèlery <sup>a</sup>, Valérie Cayol <sup>c</sup>

<sup>a</sup> Laboratoire GéoSciences Réunion, Université de la Réunion, Institut de Physique du Globe de Paris, CNRS, UMR 7154-Géologie des Systèmes Volcaniques, 15 avenue René Cassin, BP 97715 Saint-Denis cedex 9, La Réunion, France

<sup>b</sup> Observatoire Volcanologique du Piton de la Fournaise, Institut de Physique du Globe de Paris, CNRS, UMR 7154-Géologie des Systèmes Volcaniques, 14 RN3, le 27<sup>ème</sup> km, 97418, La Plaine des Cafres, La Réunion, France

<sup>c</sup> Laboratoire Magmas et Volcans, Université Blaise Pascal, CNRS, UMR 6524, Clermont-Ferrand, France

### ARTICLE INFO

#### Article history:

Received 26 February 2008

Accepted 9 September 2008

Available online 27 September 2008

#### Keywords:

Piton de La Fournaise

caldera collapse

GPS

numerical modelling

### ABSTRACT

On April 5th 2007, a major collapse of the Dolomieu summit crater occurred at Piton de La Fournaise volcano (La Réunion Island). To constrain the origin and the dynamics of the collapse, we modelled continuous GPS displacements preceding and accompanying this event. Our results reveal that the Dolomieu collapse formed by a "piston-like" mechanism, in which the fast draining of the shallow magma reservoir at the beginning of the March 30th–May 1st 2007 eruption caused a gravity-driven downward displacement of its roof. During the five days preceding the collapse, summit deflation was caused by volume change through the fractured rock column above the shallow magma chamber due to the closure of voids or small-scale cavities or the upward stopping and migration of an underground cavity. Since 2000, weakening of the rock column by repeated refilling and draining of the shallow magma chamber favoured its destabilization. On April 5th, 7 h before the onset of the collapse, the deflation source was located at ~300 m depth revealing the initiation of the collapse at very shallow depth. The sudden collapse on April 5th was followed by continuous cyclic subsidence until April 6th. Each cycle was characterized by a progressive inward deflation of the summit zone and ended by sudden summit outward displacements caused by stress relaxation following a collapse event. Subsidence of the stopped column in the magma reservoir during the collapse of the crater on April 5th and 6th acted as a piston thus increasing the eruption rate. The collapse occurred in only 24 h by successive events and increased the depth of the Dolomieu crater by 340 m. After April 6th, only minor readjustments of the summit cone occurred with slight summit deflation and small landslides of the caldera walls.

© 2008 Elsevier B.V. All rights reserved.

### 1. Introduction

Caldera and pit-crater collapses are common in the evolution of volcanic systems. These sub-circular depressions form along rift zones, Kilauea (Okubo and Martel, 1998) or at the summit of volcanoes, Piton de La Fournaise (Hirn et al., 1991; Longpré et al., 2007;

Michon et al., 2007a), Fernandina (Simkin and Howard, 1970), Miyakejima, (Geshi et al., 2002). Although the diameter of calderas and pit-craters varies from several tens of meters to several tens of kilometres, they generally result from the same mechanisms. In both cases, collapses are interpreted as the result of the emptying of magma bodies linked with magma intrusions within the edifice (Macdonald et al., 1970; Simkin and Howard, 1970; Hirn et al., 1991; Geshi et al., 2002; Longpré et al., 2007; Michon et al., 2007a).

At Piton de La Fournaise, the Dolomieu summit crater has undergone several collapses during the 19th century (Bachèlery, 1981; Carter et al., 2007). Hirn et al. (1991) and Longpré et al. (2007) described the formation of the two small pit-craters in 1986 and 2002 as the result of a pressure decrease in the magma plumbing system linked with lateral eruptions. In April 2007, it was the first time that a major collapse affecting the whole Dolomieu summit crater had been monitored by continuous GPS network at Piton de La Fournaise. From the study of continuous GPS displacements and numerical modelling, we interpret the evolution of the deformation

\* Corresponding author. Institut de Physique du Globe de Paris, CNRS, UMR 7154-Géologie des Systèmes Volcaniques, 4 place jussieu, Paris, France. Tel: +33 1 44 27 84 83; fax: +33 1 44 27 73 85.

E-mail addresses: [peltier@ipgp.jussieu.fr](mailto:peltier@ipgp.jussieu.fr) (A. Peltier), [Thomas.Staudacher@univ-reunion.fr](mailto:Thomas.Staudacher@univ-reunion.fr) (T. Staudacher), [Patrick.Bachelery@univ-reunion.fr](mailto:Patrick.Bachelery@univ-reunion.fr) (P. Bachèlery), [V.Cayol@opgc.univ-bpclermont.fr](mailto:V.Cayol@opgc.univ-bpclermont.fr) (V. Cayol).

<sup>1</sup> Present address: Institut de Physique du Globe de Paris, CNRS, UMR 7154-Géologie des Systèmes Volcaniques, 4 place jussieu, Paris, France.

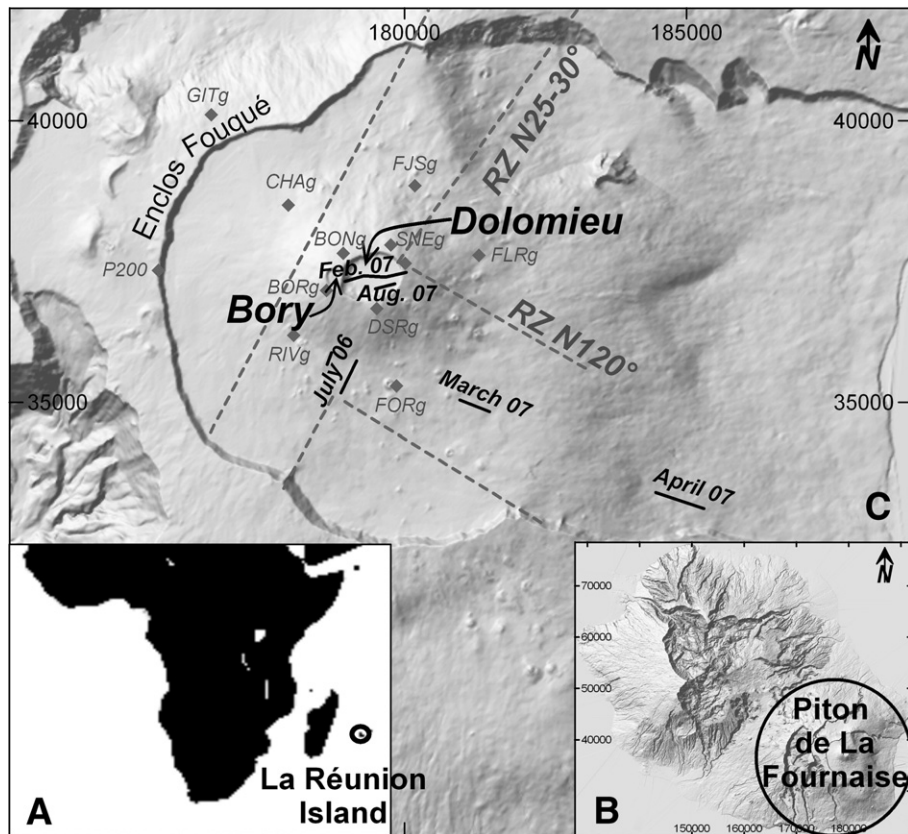


**Fig. 1.** Location maps of (A) La Réunion Island, and (B) Piton de La Fournaise volcano. (C) Location of rift zones (grey dotted lines, after Michon et al., 2007b), 2006–2007 eruptive fissures (black lines) and permanent GPS stations (diamonds). (Gauss Laborde Réunion coordinates, in meters).

source preceding the April 2007 collapse in order to explain its origin and dynamics.

## 2. Geological setting of Piton de La Fournaise

### 2.1. General view

Piton de la Fournaise is the active volcano of La Réunion Island, located in the SW part of the Indian Ocean (Fig. 1A,B). A 400 m high summit cone, 3 km wide at its base, has been built in the central part of the Enclos Fouqué caldera. Two craters cut the summit of this cone: Dolomieu crater in the East and Bory crater in the West (Fig. 1C). The eruptive activity typically takes place inside the Dolomieu crater or along two preferential feeding pathways striking N25–30° and N120° (Michon et al., 2007b; Fig. 1c). Three types of eruption can be distinguished (Peltier, 2007): (1) summit eruptions taking place in Dolomieu crater; (2) proximal eruptions beginning with the opening of fissures migrating downslope on the central cone flanks; (3) distal eruptions occurring outside of the summit cone, more than 4 km from the summit. The recent summit pit-crater and caldera collapses were directly related to the distal eruptions which emit large volume of lava flows, between 15 and 140 Mm<sup>3</sup>, much larger than volumes of 1–20 Mm<sup>3</sup> typical of the summit and proximal eruptions (Bachèlery, 1981; Lénat et al., 1989; Hirn et al., 1991; Longpré et al., 2007; Michon et al., 2007a). The most recent collapses in Dolomieu crater occurred between 1931 and 1935 (east), in 1953 (southwest), in 1961 (southwest), in 1986 (southeast), in 2002 (southwest) and in 2007 (all of the Dolomieu crater). Collapses of the Dolomieu crater alternated with its re-fillings by lava accumulations during summit eruptions (Bachèlery, 1981). At the end of 2006, the eastern part of Dolomieu was fully filled.

### 2.2. Summary of the recent activity of Piton de La Fournaise

#### 2.2.1. The 1998–2007 period of activity

After 6 yr of repose, 25 eruptions and one intrusion occurred between 1998 and 2007. Since 2000, five eruptive cycles have been defined: 2000–January 2002 (4 eruptions), May 2003–January 2004 (4 eruptions and 1 intrusion), May 2004–February 2005, October 2005–January 2006 (3 eruptions) and July 2006–May 2007 (4 eruptions). Each eruptive cycle began with summit or proximal eruptions and ended by a major distal eruption, with successive eruptive vents opening lower and lower on the volcano flanks in few months (Peltier, 2007; Peltier et al., 2008).

#### 2.2.2. The 2006–2007 eruptive cycle

The 2006 and 2007 years were characterized by a quasi-continuous eruptive activity with 4 eruptions in 10 months: the July–August 2006 proximal eruption, the August 2006–January 2007 summit eruption, the February 2007 summit eruption and the March–May 2007 distal eruption. Each of these four eruptions was only separated by 2 to 7 weeks of repose. The first three eruptions occurred at high elevation (inside the Dolomieu crater or at the base of the summit cone; Fig. 1C) and were characterized by low volumes of lava flows and low effusion rates (0.5–20 Mm<sup>3</sup> and 1.2–15 m<sup>3</sup> s<sup>-1</sup>, respectively). The August 2006–January 2007 eruption was the longest eruption since 1998, with four months of continuous activity, and emitted around 20 Mm<sup>3</sup> of lava flows, 10 times larger than typical summit eruptions. At the end of this event, the height of the Dolomieu crater floor had increased by 30 m due to lava flow accumulation.

The 2006–2007 eruptive cycle ended with the March–May 2007 distal eruption, which took place in two phases. The first phase began on March 30th at 18:50 (UTM) after a seismic crisis of 2.5 h. The eruptive fissure was located at 1900 m elevation at the base of the south-eastern part of the central cone (Fig. 1C). Eruptive tremor ceased

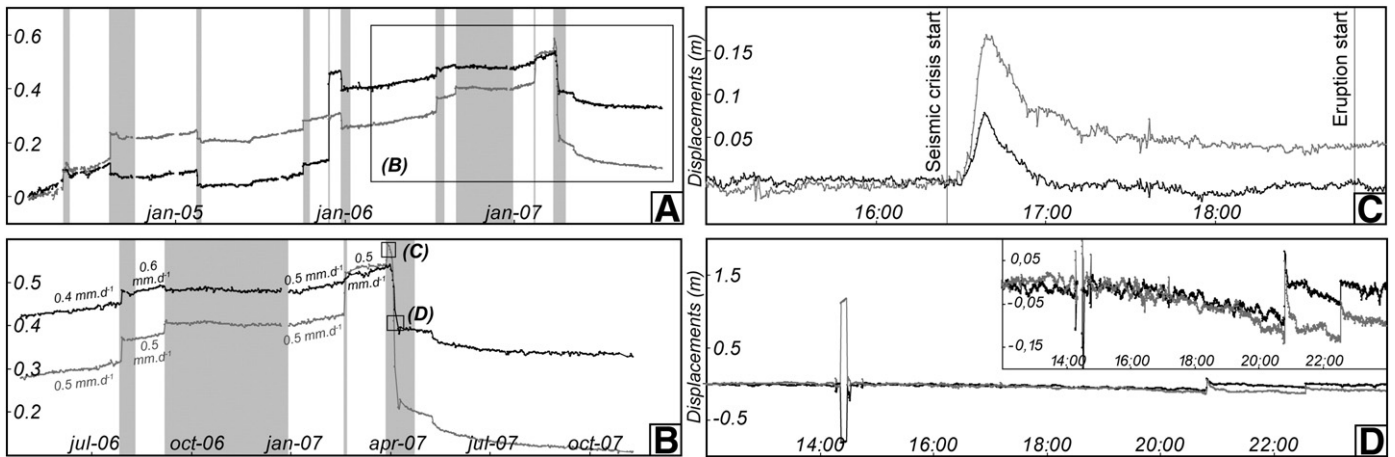


**Fig. 2.** Cumulative horizontal displacements (black: EW component, grey: NS component) recorded on the SNEg summit GPS station. Data windows (A) between 2004 and 2007, (B) during the 2006–2007 eruptive cycle, (C) during the March 30th 2007 magma migration, (D) and at the beginning of the Dolomieu collapse on April 5th 2007 (the displacement scale is enlarged in the inset). Shaded areas represent eruptive periods.

on March 31st at 05:15 after the emission of less than  $1 \text{ Mm}^3$  of lava. At the end of this short phase, seismicity persisted below the summit craters at  $1\text{--}2 (\pm 0.3) \text{ km}$  depth but also below the eastern flank at  $3.5\text{--}4.5 (\pm 0.3) \text{ km}$  depth. On April 2nd at 06:00, a new eruptive phase started at low elevation ( $\sim 600 \text{ m}$ ) on the south-eastern flank, 7 km away from the summit (Fig. 1C). April 6th corresponds to a paroxysmal phase during which 200 m high lava fountains were observed at the eruptive vent. This increase of activity was accompanied with an increase of eruptive tremor. The main Dolomieu crater collapse was observed for the first time in the afternoon of April 6th when the weather allowed field observations. No large ash emissions were observed. The eruptive tremor progressively decreased after April 6th at 16:00. After a short break of 8 h on April 10th, the eruption continued until May 1st accompanied by minor collapses and landslides that progressively enlarged the volume of the Dolomieu crater ( $90 \text{ Mm}^3$ ; Michon et al., 2007a; Urai et al., 2007; Staudacher et al., 2009-this issue). The effusion rate and the total volume of lava flows have been estimated at  $\sim 54 \text{ m}^3 \text{ s}^{-1}$  and  $\sim 130\text{--}140 \text{ Mm}^3$ , respectively (Staudacher et al., 2009-this issue); the largest values observed since the establishment of the observatory in 1980. The whole 2006–2007 eruptive cycle was characterized by high volume of lava, around  $165 \text{ Mm}^3$  compared to a mean of  $34 \text{ Mm}^3$  during the previous cycles.

### 3. GPS measurements of ground displacements

#### 3.1. GPS network

Since 1980, the Piton de La Fournaise activity has been monitored by seismic and deformation networks of the Volcanological Observatory of Piton de La Fournaise. The continuous GPS network is equipped since 2004 with ten stations and two reference stations (P200 and GITg; Fig. 1C). Each GPS station consists of Ashtech Zxtrem, Trimble NetRS or Topcon GB-1000 installed on stainless steel rods cemented in the bedrock or on concrete pillars. Data are acquired at 30 s intervals. The position of each station is calculated relative to the reference stations using the Winprism software. In addition to the permanent GPS network, the position of 80 stainless steel benchmarks are measured by kinematic GPS campaigns immediately after each eruption with an acquisition time of 7 min at each station and a sampling rate of 1 measurement per sec.

#### 3.2. Ground deformation behaviour at Piton de la Fournaise

Two time scales of ground deformation are recorded at Piton de La Fournaise (Peltier, 2007; Peltier et al., 2008).

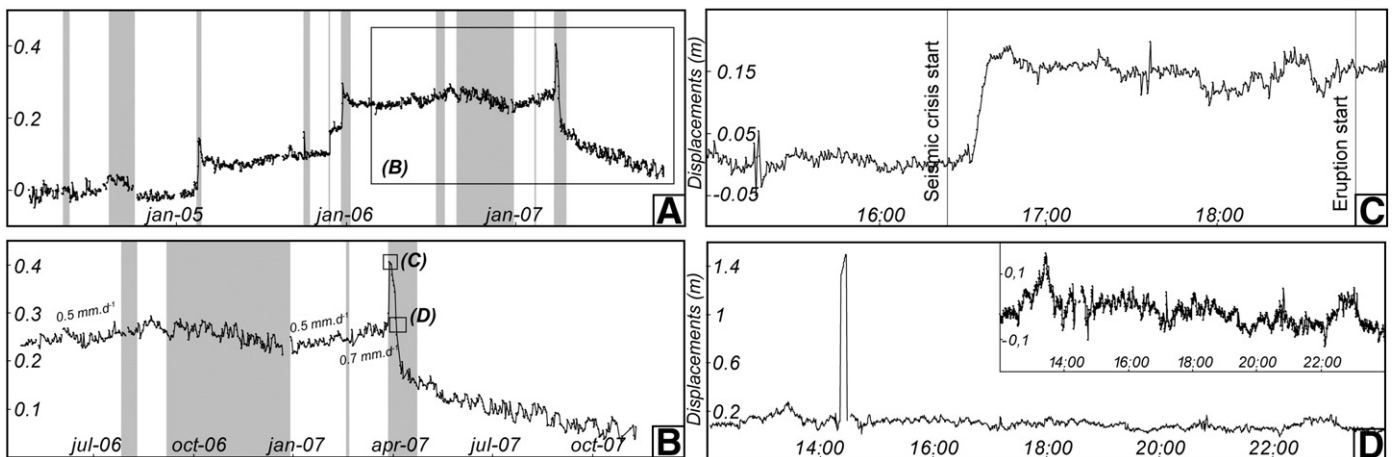


**Fig. 3.** Cumulative vertical displacements recorded on the SNEg summit GPS station. Data windows (A) between 2004 and 2007, (B) during the 2006–2007 eruptive cycle, (C) during the March 30th 2007 magma migration, (D) and at the beginning of the Dolomieu collapse on April 5th 2007 (the displacement scale is enlarged in the inset). Shaded areas represent eruptive periods.

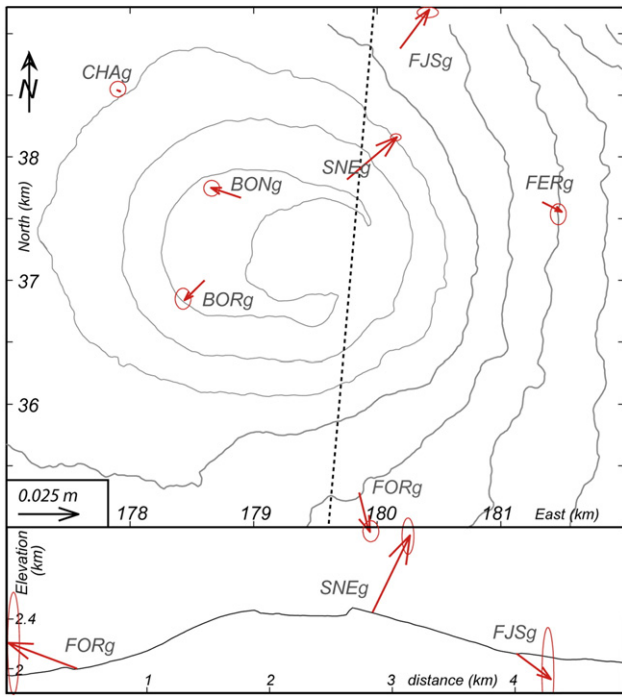


**Fig. 4.** Cumulative displacements recorded on the permanent GPS network between February 21st and March 29th 2007. Error ellipses are shown. (Gauss Laborde Réunion coordinates).

(1) Since the appearance of eruptive cycles in 2000, small long-term ground displacements are systematically recorded during inter-eruptive periods. Between 2 weeks and 5 months before each eruption a slight summit inflation occurs ( $0.4\text{--}0.7\text{ mm day}^{-1}$ ); whereas a post-eruptive summit deflation lasting 1 to 3 months is only recorded after the largest distal eruptions ( $0.3\text{--}1.3\text{ mm day}^{-1}$ ; Figs. 2A and 3A).

(2) The largest displacements, reaching up to  $20 \times 10^3\text{ mm day}^{-1}$ , are monitored a few min to hours prior each eruption during magma injections toward the surface (Figs. 2A and 3A).

3.3. GPS displacements linked with the 2006–2007 eruptive cycle

The evolution of GPS displacements recorded on the SNEg station during the 2006–2007 eruptive cycle is shown on Figs. 2B and 3B. The 2006–2007 eruptive cycle displayed the typical long-term pre-eruptive summit inflation described above. At the end of March 2006, summit inflation started and was only interrupted by short-term ground displacements linked with the eruptions of July–August 2006, August 2006–January 2007 and February 2007 (Figs. 2B and 3B). Immediately after each of these eruptions, summit inflation resumed at the same rate for the EW and NS components,  $0.4\text{--}0.6\text{ mm day}^{-1}$  and  $0.4\text{--}0.5\text{ mm day}^{-1}$ , respectively (Peltier et al., 2008), but at distinct rate for the vertical component. During the two weeks of repose between the July–August 2006 and the August 2006–January 2007 eruptions, the summit displacements were purely horizontal (Figs. 2B and 3B). Whereas the vertical displacement rates increased ( $0.7\text{ mm day}^{-1}$  on SNEg) before the March–May 2007 eruption (Figs. 3B and 4), as observed before the distal eruptions of the 2004–2005 cycles (Peltier et al., 2008).

3.4. GPS displacements linked with the March–May 2007 distal eruption

3.4.1. Dynamics of magma injection

The chronology of GPS displacements linked with the March–April 2007 magma injection is as follows:

- (1) Between 16:25 and 16:40, on March 30th, a short summit inflation lasting ~15 min was recorded on the summit GPS stations (Figs. 2C, 3C and 5A).
- (2) After 16:40, the summit GPS stations started to record summit contraction but only little subsidence, whereas the stations located at the base of the cone (FJSg, FORg, FERg) recorded the first signs of displacements toward the south-eastern flank of

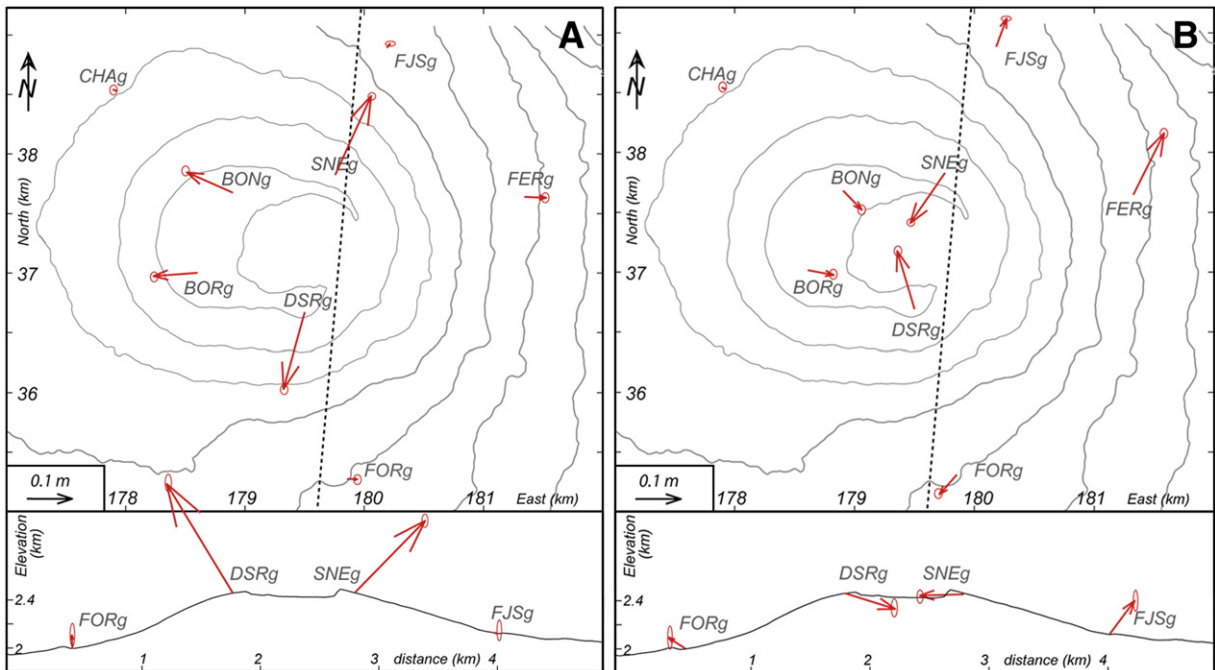


**Fig. 5.** Cumulative displacements recorded on the permanent GPS network during the March 30th 2007 magma injection, (A) between 16:25 and 16:40 and, (B) between 16:40 and 18:50. Error ellipses are shown. (Gauss Laborde Réunion coordinates).

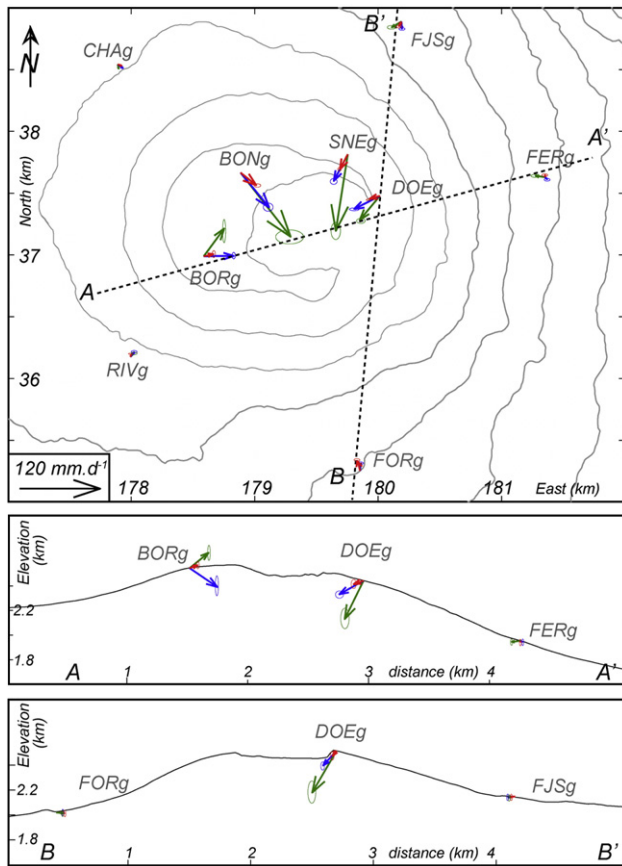


**Fig. 6.** Displacement rates recorded on the permanent GPS network between April 2nd and 5th (red), between April 5th and 6th (green) and between April 6th and 10th (blue). Error ellipses are shown. (Gauss Laborde Réunion coordinates). (For interpretation of the references to color in this figure legend, the reader is referred to the web version of this article.)

the volcano linked with the growth of a lateral dyke (Figs. 2C, 3C and 5B). Note that between 16:40 and 17:15, strong displacements were also recorded on the FJSg GPS station located on the northern flank (Fig. 5B). Following 10 h of eruptive activity on March 30th and 31st, a slight summit deflation persisted (Figs. 2C and 3C). On April 2nd, the opening of a new eruptive fissure at 600 m of elevation did not disrupt the displacement trends recorded by the GPS stations located around the summit cone, 7 km from the fissure.

#### 3.4.2. Dynamics of the Dolomieu crater subsidence and collapse

GPS displacements preceding and following the 2007 Dolomieu collapse are shown on Figs. 6 and 7. Unfortunately, the station located on the southern rim of Dolomieu crater (DSRg) did not work. Several stages can be distinguished before, during, and after the main collapse of April 5th.

- (1) March 30th–April 5th (on SNEg station, displacement rates of  $-6$ ,  $-12$ , and  $-13$   $\text{mm day}^{-1}$ , on the EW, NS, and vertical components, respectively; Figs. 2B, 3B and 6). Following the March 30th magma injection all GPS stations, except BORg, recorded subsidence. The BORg station, located west of Bory crater, recorded a slight uplift until April 5th (Fig. 6). The ground displacements extended outside of the Enclos Fouqué caldera with significant displacements recorded on GITg station (Fig. 1). The EW and NS components of the GITg station recorded displacement rates toward the summit cone of  $0.8$   $\text{mm day}^{-1}$ ,  $-1.2$   $\text{mm day}^{-1}$ , respectively from March 30th to April 10th

- (2) April 5th–6th (on SNEg station, displacement rates of  $-19$ ,  $-121$ , and  $-58$   $\text{mm day}^{-1}$ , on the EW, NS, and vertical components, respectively; Figs. 2B, 3B and 6). On April 5th, a quick inward displacement of the whole summit zone was recorded (Figs. 2D and 3D), after a 6-minute period of highly perturbed GPS displacements between 14:22 and 14:28. The increase of deflation began with an increase of eruptive tremor and was recorded on the whole GPS network, with the largest signal recorded on the stations located around the Dolomieu crater. At 20:48, sudden outward displacements of 10–20 cm were recorded on the GPS summit stations (Figs. 2D and 3D). This global outward motion on the summit occurred at the same time as a 3.2 Md earthquake. After this event, cycles of deformation occurred until April 6th. Each cycle was characterized by progressive inward displacements ending in a strong outward motion (Figs. 2D and 3D). These deformation cycles were contemporaneous with the onset of seismic cycles that included increases of tremor (Michon et al., 2007a). The sudden collapse of the Dolomieu crater occurred during this strong summit deflation, and was first observed in the afternoon of April 6th.
- (3) April 6th–10th (on SNEg station, displacement rates of  $-22$ ,  $-43$ , and  $-22$   $\text{mm day}^{-1}$ , on the EW, NS, and vertical components, respectively; Figs. 2B, 3B and 6). After April 6th, the summit deflation persisted but at lower rates.

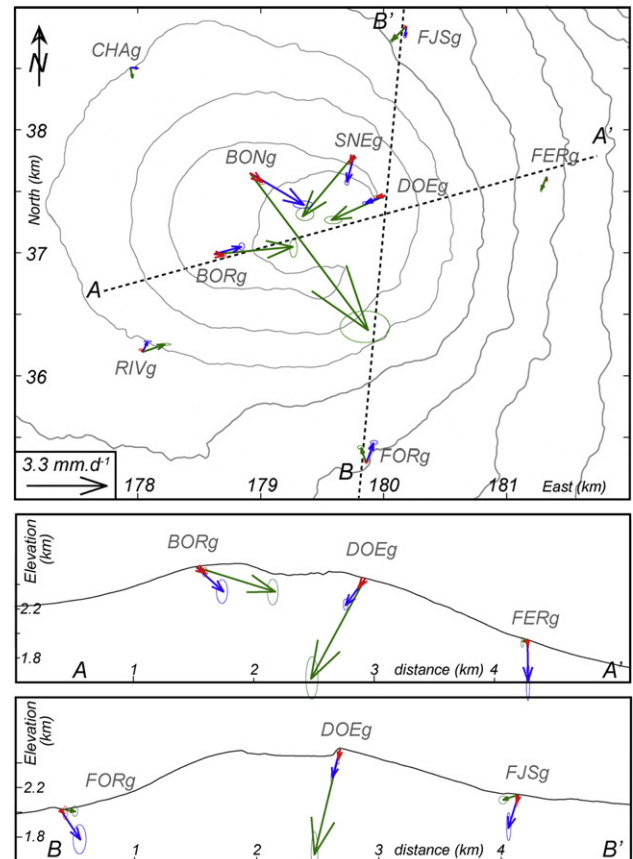


**Fig. 7.** Displacement rates recorded after the major Dolomieu collapse on the permanent GPS network between April 10th and May 12th (red), between May 13th and 20th (green) and between May 20th and October 30th (blue). Error ellipses are shown. (Gauss Laborde Réunion coordinates). (For interpretation of the references to color in this figure legend, the reader is referred to the web version of this article.)

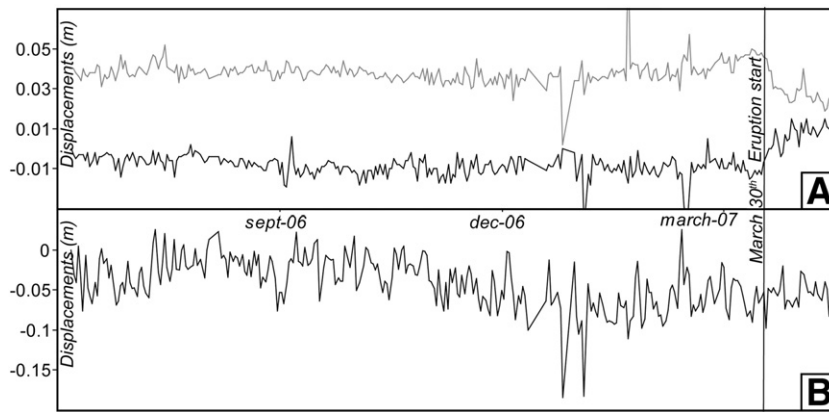


**Fig. 8.** (A) Cumulative horizontal (black: EW component, grey: NS component) and (B) vertical displacements recorded at the GIfg permanent GPS station in 2006 and 2007.

- (4) April 10th–May 12th (on SNEg station, displacement rates of  $-0.3$ ,  $-1.1$ , and  $-0.9$   $\text{mm day}^{-1}$ , on the EW, NS, and vertical components, respectively; Figs. 2B, 3B and 7). Following a short break of 8 h in the eruptive activity on April 10th, the summit deflation slowed down again until March 12th.
- (5) May 12th–20th (on SNEg station, displacement rates of  $-2.1$ ,  $-2.5$ , and  $-3.2$   $\text{mm day}^{-1}$ , on the EW, NS, and vertical components, respectively; Figs. 2B, 3B and 7). On May 12th, a 10 min subterranean collapse event highlighted by seismic records occurred. An increase of subsidence and inward displacements accompanied this event and persisted until May 21st.
- (6) After May 21st (on SNEg station, displacement rates of  $-0.4$ ,  $-0.6$ , and  $-0.1$   $\text{mm day}^{-1}$ , on the EW, NS, and vertical components, respectively; Figs. 2B, 3B and 7). Low deflation rates continued until June 2008, with essentially horizontal contractions toward the Dolomieu crater centre (Figs. 2B, 3B and 7). This was the longest period of unrest without summit inflation since 2000.

For each stage, the horizontal GPS vector displacements were always radial and converged toward the Dolomieu crater centre (Figs. 6 and 7) and subsidence rates decreased between the summit and the base of the cone. On a larger spatial scale, kinematic GPS measurements recorded between March and May 2007 show that the influence of the Dolomieu collapse was weak at the base of the cone (Fig. 9). The base of the cone was mostly influenced by the dyke propagation toward the south-eastern flank.

#### 4. Numerical modelling

Numerical modelling is used to constrain the pressure sources that can explain the observed ground displacements preceding and associated with the April 2007 Dolomieu collapse. GPS data are used as an input in a three dimensional elastic model based on the mixed boundary element method (Cayol, 1996; Cayol and Cornet, 1997). The model is combined with Sambridge's Monte Carlo inversion method (Sambridge, 1999a) to minimize the misfit function (Fukushima et al., 2005), i.e. the normalized root mean square error between calculated and observed displacements. For the calculation, the edifice is assumed to be elastic, homogeneous and isotropic, with a Young's modulus of 5 GPa, and a Poisson's ratio of 0.25 (Cayol, 1996). The structures (topography and pressure sources) are modelled by meshes with triangular elements. Surface displacements are calculated at the summits of the mesh elements. Long-term ground displacements are modelled from GPS data by ellipsoidal over/under-pressurized sources ( $\Delta P$ ). Ellipsoids are defined by 7 parameters: the 3D coordinates of its centre, the dimensions of its three half axes and  $\Delta P$ . Confidence intervals on these parameters are estimated from a one dimensional posterior probability density function (Sambridge, 1999b).

##### 4.1. The February–March 2007 pre-eruptive inflation

The summit inflation preceding the March–May 2007 eruption can be explained at 74% by an ellipsoidal pressure source ( $\Delta P = 3.5 \pm$

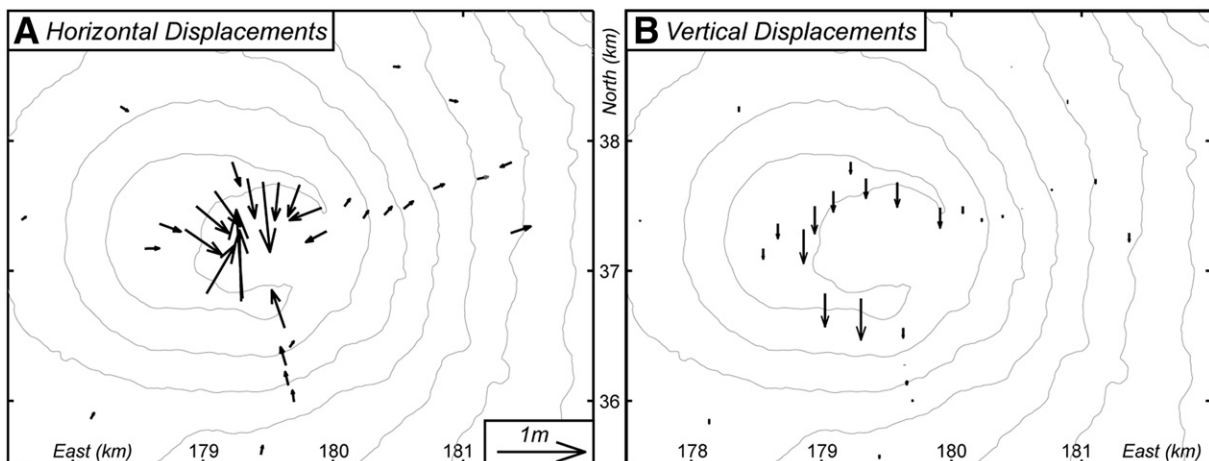


**Fig. 9.** Cumulative GPS displacements recorded between March (14th, 19th, 21st, 22nd) and May 2007 (10th, 21st, 24th) by kinematic measurements. Errors on measurements are around 0.02 m and 0.2 m on the horizontal and vertical components, respectively. (Gauss Laborde Réunion coordinates).

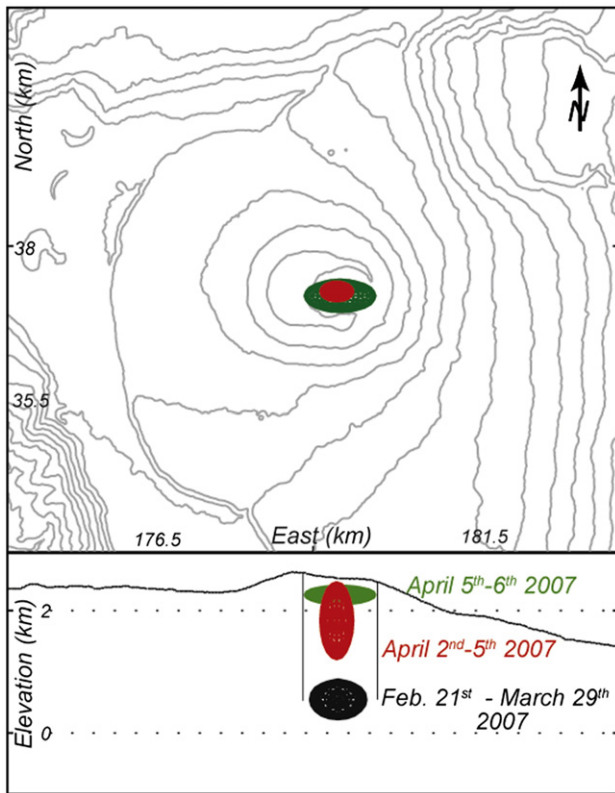


**Fig. 10.** Location of the sources modelled for the February–March 2007 pre-eruptive inflation (black) and for the deflation periods of April 2nd–5th (red) and April 5th–6th 2007 (green). Black lines represent the fractures involved in the second set of modelling (Fig. 12) (Gauss Laborde Réunion coordinates). (For interpretation of the references to color in this figure legend, the reader is referred to the web version of this article.)

0.4 MPa and  $\Delta V = 0.5 \pm 0.1 \text{ Mm}^3$ ) located beneath the Dolomieu crater at  $460 \pm 400 \text{ m}$  elevation (Figs. 10, 11A and 12A; Table 1).

#### 4.2. The March–April 2007 magma injection

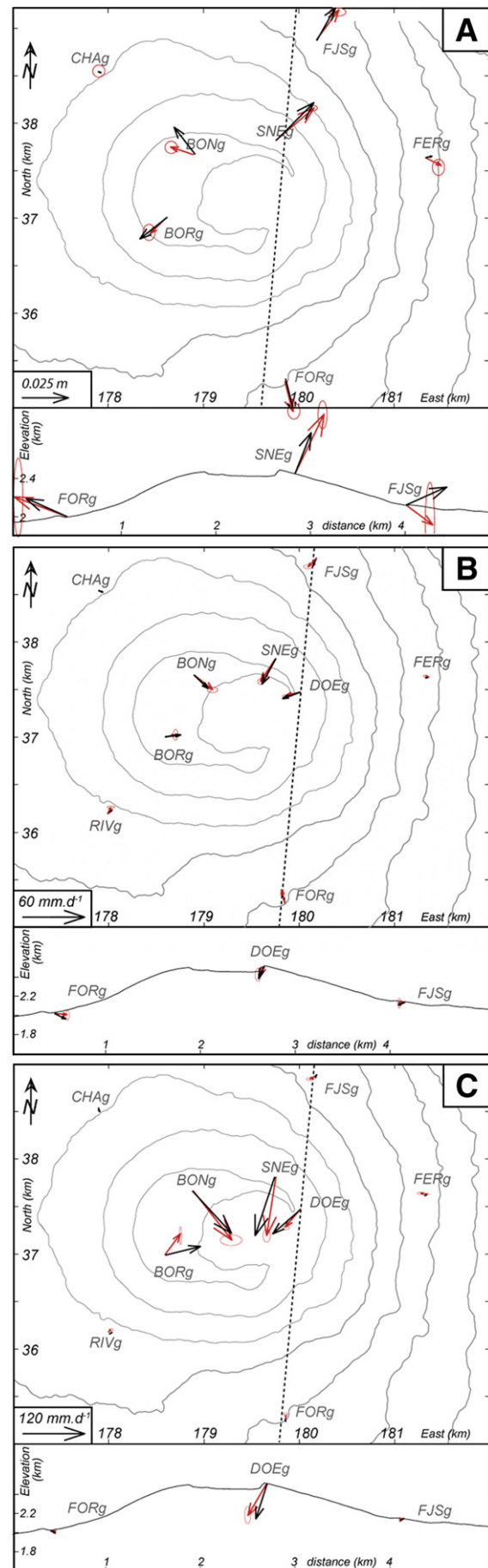
The lack of GPS data outside the cone and the strong influence of the summit deflation on the kinematic GPS measurements prevent us from modelling the dyke that fed the March–April 2007 distal eruption. However, considering the continuous summit deflation between March 30th and April 2nd and the alignment of eruptive fissures (Fig. 1c), we assume that only one dyke, starting below the Dolomieu crater fed the two eruptive fissures on March 30th and April 2nd. To explain the strong displacements recorded on the FJSg station during the first minutes of the seismic crisis, we suppose that a second dyke fed a short magma intrusion toward the north.

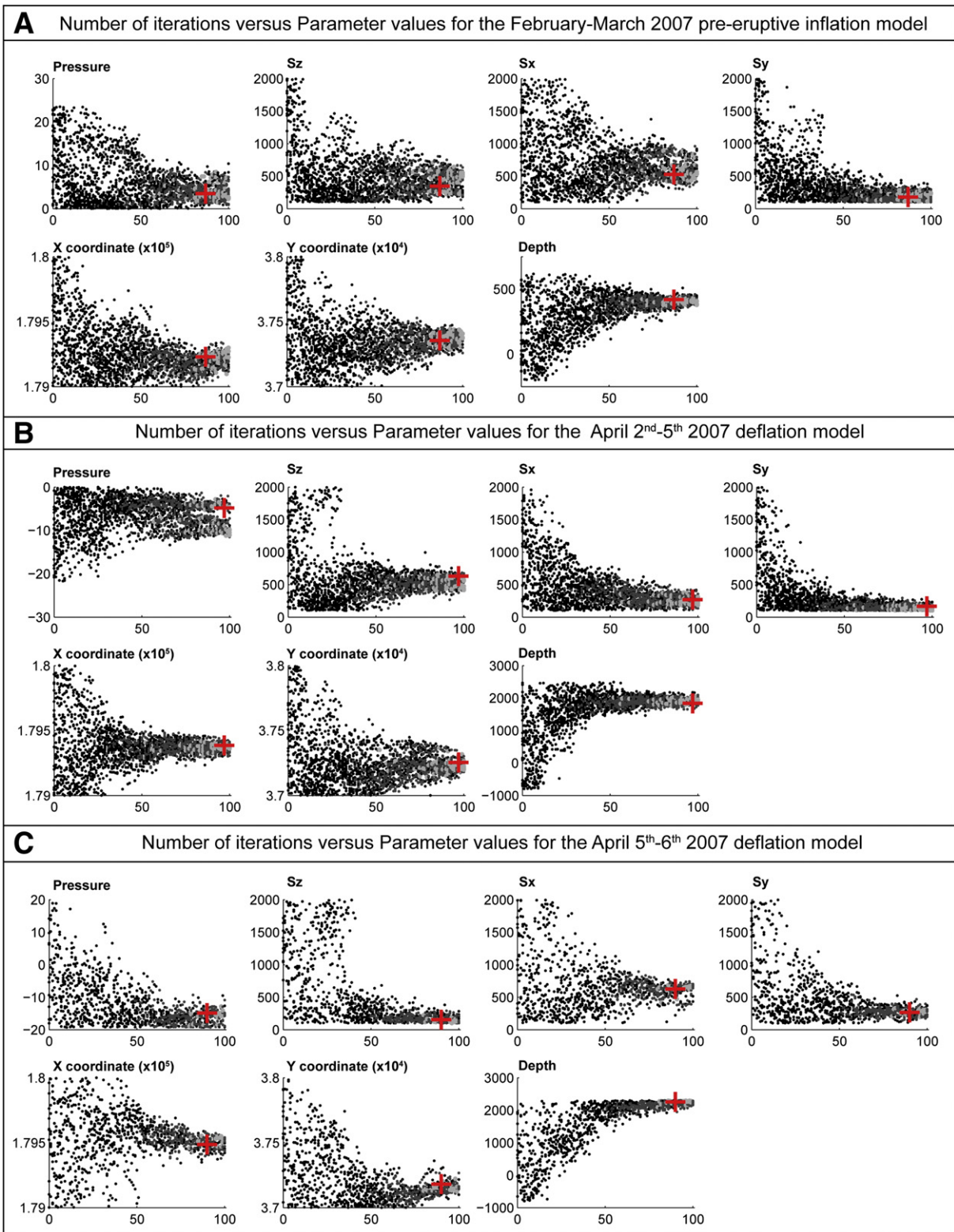
#### 4.3. The April 2007 subsidence

Fig. 10 shows the geometry of under-pressurized sources that best explains the displacements associated with the two stages of summit deflation, April 2nd–5th and April 5th–6th, preceding the Dolomieu crater collapse.

Between April 2nd and 5th, GPS displacements can be explained at 87% by a deflation source ( $\Delta P = -4.8 \pm 1.6 \text{ MPa}$  and  $\Delta V = -1 \pm 0.3 \text{ Mm}^3$ )

**Fig. 11.** Comparison between observed (red) and calculated (black) displacements for the (A) February–March 2007 pre-eruptive inflation and for the deflation periods of (B) April 2nd–5th and (C) April 5th–6th 2007. (Gauss Laborde Réunion coordinates). (For interpretation of the references to color in this figure legend, the reader is referred to the web version of this article.)





**Fig. 12.** Number of iterations versus parameter values for (A) the February–March 2007 pre-eruptive inflation model, (B) the April 2<sup>nd</sup>–5<sup>th</sup> 2007 deflation model, and (C) the April 5<sup>th</sup>–6<sup>th</sup> 2007 deflation model.

that extended from 1150 to  $2300 \pm 350$  m elevation (Figs. 10, 11B and 12B). In contrast, on April 5<sup>th</sup> and 6<sup>th</sup> the strongest ground displacements can be explained at 89% by a shallow source ( $\Delta P = -15 \pm 5$  MPa and  $\Delta V = -1.46 \pm 0.5$  Mm<sup>3</sup>) located just below the surface at 2250  $\pm$  420 m elevation (Figs. 10, 11C and 12C; Table 1).

#### 4.4. Influence of the fractures on the ground deformation

Caldera collapse formation involves discontinuities at depth and most often caldera collapses are controlled by pre-existing concentric fractures (Roche et al., 2001; Cole et al., 2005; Acocella and Tibaldi,

**Table 1**  
Summary of the modelled pressure sources parameters.

Models	Sz (m)	Sx (m)	Sy (m)	X	Y	Z	$\Delta P$ (MPa)	$\Delta V$ ( $\times 10^6$ $m^3$ )	Consistency (%)
Feb. 21st– March 29 <sup>th</sup>	352	526	280	179,229	37,300	460	3.5	0.5	74
April 2nd–5th	575	269	166	179,385	37,254	1737	−4.8	−1.0	87

2007). De Natale and Pingue (1993) and Letourneur et al. (2008) suggested that discontinuities control ground deformation distribution. A pressure source in a heterogeneous medium characterized by structural discontinuities produces deformation over a smaller area with respect to a continuous medium, mostly because some of the deformation is accommodated by inelastic structures.

To test the influence of pre-existing fractures on pre-collapse ground deformation, we have included in a set of models sub-vertical fractures around the Dolomieu crater extending from the shallow reservoir (420 m elevation) to the surface according to analogue experiments of Roche et al. (2001). Fig. 13 compares the ground deformation on the GPS sites induced by pressure sources in homogeneous and fractured medium. Permanent GPS stations are located just outside of the ring delimited by the main fractures generating the collapse (Michon et al., 2009-this issue; Fig. 13). For the pre-eruptive inflation, the pressure source is located just below the fractures (Fig. 10) and our results show an increase of summit ground deformation by ~20% around the pre-collapse fractures relative to a homogeneous medium, whereas no significant change occurs at the base of the summit cone (Fig. 13A). By contrast, when the pressure source is located inside the fault network (Fig. 13B, C), summit ground deformation decrease compared to a homogeneous medium, mostly because some of the deformation is accommodated by slip motion of the surrounding fractures. Consequently, the assumption of a homogeneous medium in our numerical modelling can lead to an underestimation (pre-eruptive inflation source below the fault network) or an overestimation (deflation source bordered by fault network) of the depth of pressure sources. Because we are unable to constrain with precision the size, number, and location of discontinuities at depth, we conclude that the depths of our deflation sources, previously modelled, represent only minimum depths (Fig. 10). However we can easily deduce from our numerical modelling that the location of the deflation sources were distinct from April 2nd and 6th and allows us to interpret the processes leading to the Dolomieu crater collapse on April 5th, 2007.

## 5. Discussion

### 5.1. Origin of the collapse

The April 2007 Dolomieu collapse started 6 days after the onset of the March–May 2007 distal eruption (Fig. 6). The lack of large pyroclastic emissions excludes explosive mechanisms to explain the collapse. Instead, the Dolomieu collapse was linked with the fast draining of the shallow magma reservoir (see pre-eruptive inflation source on Fig. 10 for location), considering the large volume of erupted lava and the high emission rate of this eruption (estimated at  $\sim 130$ – $140 \times 10^6 m^3$  and  $\sim 54 m^3 s^{-1}$ , respectively). The rapid pressure decrease inside the magma reservoir caused a gravity-driven downward displacement of its roof. The radial ground displacements preceding and accompanying the collapse were limited to the margins of the Dolomieu crater. The base of the cone did not suffer from major

displacements (Fig. 6). We interpret this to mean that the stress concentration at the roof margin was the result of underground cavity and the Dolomieu collapse formed by a “piston-like” mechanism (Roche et al., 2001).

The volume of the Dolomieu collapse was 1.4 times greater than the volume of lava that had been erupted at the onset of the collapse on April 5th ( $56 Mm^3$  emplaced as lava flows between April 2nd and April 5th and  $10 Mm^3$  emplaced in the dyke, Staudacher et al., 2009-this issue). Two hypotheses might explain this discrepancy (Michon et al., 2007a):

- (1) a large amount of magma had intruded the edifice without reaching the surface;
- (2) the collapse had been initiated at depth before the beginning of the March–May 2007 eruption.

The first hypothesis is supported by the strong ground displacements recorded on FJSg GPS station (Fig. 5B) and the seismicity toward the north-eastern flank at the beginning of the March 30th magma injection (between 16:40 and 17:15).

However, there is also evidence to support the second hypothesis. The change of the volcano behaviour in 2000 (long-term summit inflation accompanied by an increase of long-term pre-eruptive seismicity) could indicate the initiation of the collapse at depth a few years before its appearance in surface. The long-term summit inflation has been interpreted as due to a quasi-continuous refilling of the shallow magma reservoir, explaining thus the large volume of erupted magma since 2000, notably during the 2006–2007 eruptive cycle (Peltier, 2007; Peltier et al., 2008). The successive eruptions occurring between 2000 and 2007 contributed to a progressive weakening and destabilization of the host rock column located above the magma reservoir. The weakening of the rock column created by inflations/deflations since 2000, had made the edifice unstable, allowing thus a smaller amount of magma withdrawal to form a larger volume caldera, similar to the 1968 collapse at Fernandina, Galapagos (Simkin and Howard, 1970; Munro and Rowland, 1996).

### 5.2. Chronology of the 2007 Dolomieu collapse

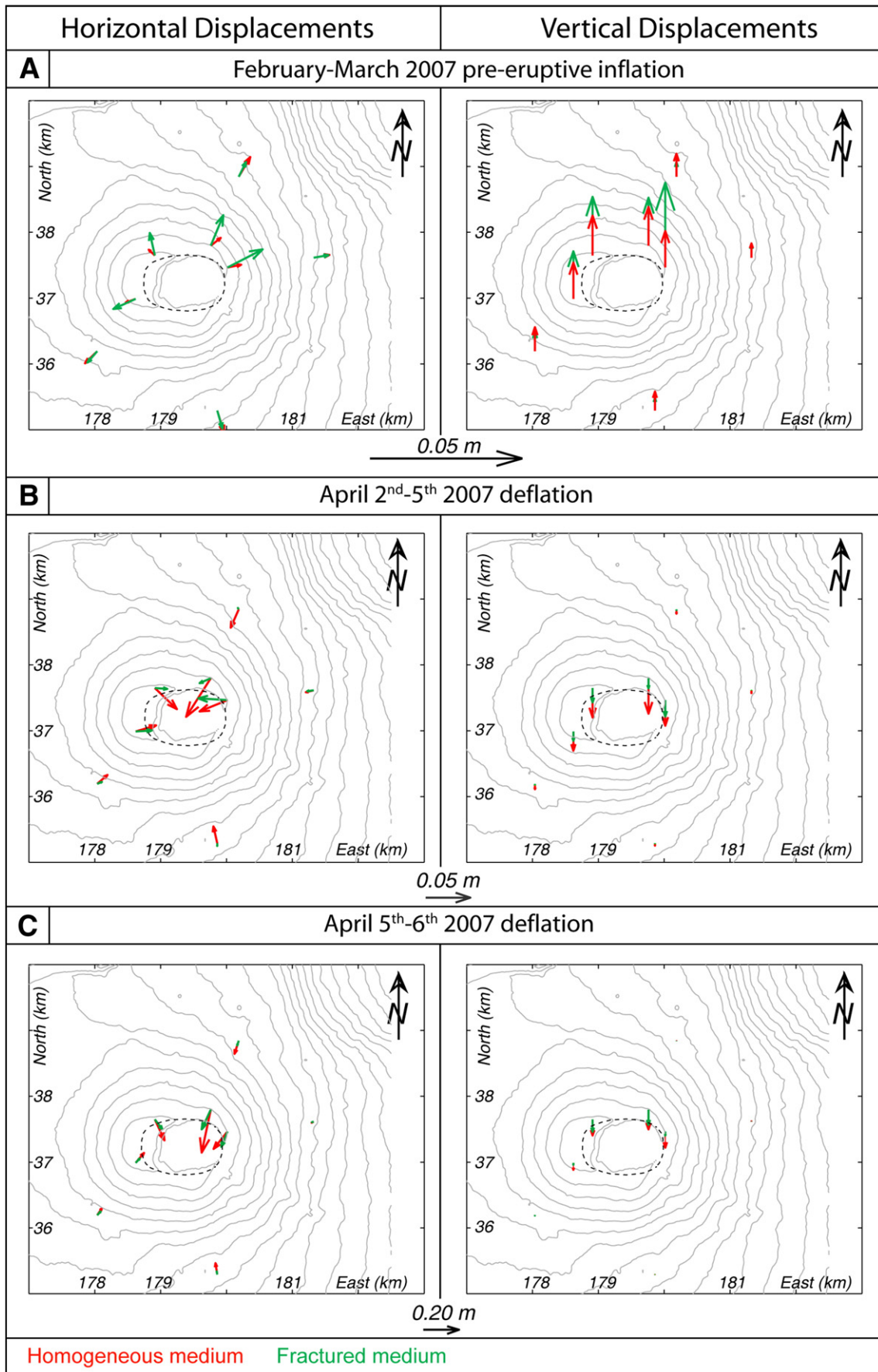
Roche et al. (2001) proposed a “piston-like” mechanism for summit pit-crater/caldera formation. In the case of Piton de La Fournaise, the reservoir roof has an aspect ratio (roof thickness/roof width) of 2–2.5 (Fig. 10). According to Roche et al. (2001), in analogue experiments with an aspect ratio of 2, collapse is non-coherent, restricted to deeper levels, and occurs without significant surface subsidence. This stage would correspond to the 2000 and 2007 period with the progressive destabilization of the rock column above the magma reservoir.

The sudden surface collapse occurred in April 2007 during a major distal eruption. For the first time since the installation of the GITG GPS station, the ground deformation extended outside of the Enclos Fouqué caldera (Fig. 8). This larger ground deformation distribution could reflect a deeper pressure source and/or the involvement of a larger volume of magma at depth, thus favouring a major distal eruption. The fast draining of a large volume of magma from the shallow reservoir allowed the failure of the roof rock when the gravitational stress exceeded its strength.

#### 5.2.1. March 30th April 5th: summit deflation

The final mechanism of the Dolomieu collapse is schematically illustrated on Fig. 14. On March 30th, after 15 min of strong summit inflation (Figs. 2C and 5A) linked with magma migration below the Dolomieu crater (Fig. 14A), a summit contraction was recorded (Figs. 2C and 5B) due to the intrusion of the dyke toward the flank (Fig. 14B).

**Fig. 13.** Comparison between ground deformation induced by pressure sources in homogeneous (red) and fractured medium (green) for (A) February–March 2007 pre-eruptive inflation (B) April 2nd–5th 2007 deflation and (C) April 5th–6th 2007 deflation. Modelled fractures are marked by dotted black lines. (Gauss Laborde Réunion coordinates). (For interpretation of the references to color in this figure legend, the reader is referred to the web version of this article.)



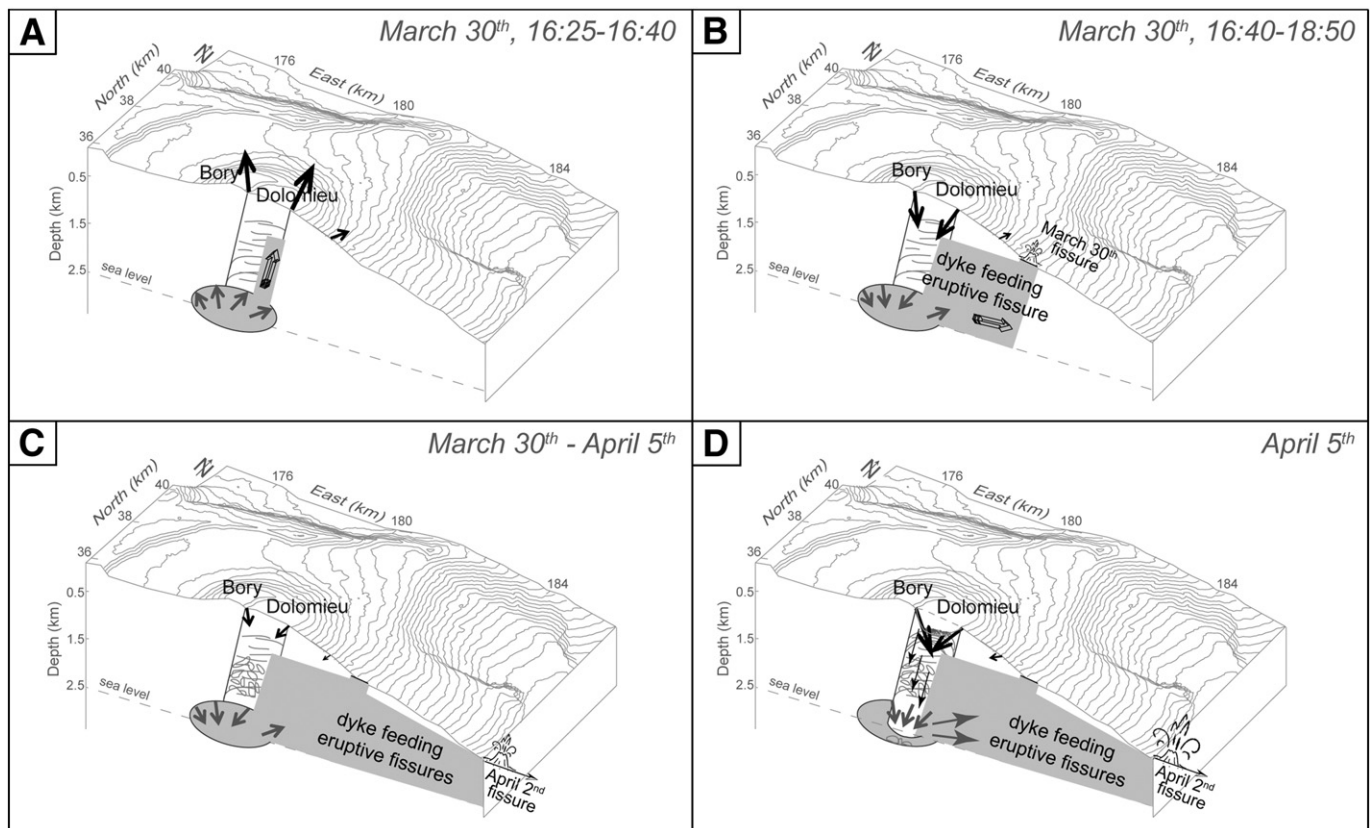


**Fig. 14.** Schematic representation of the Dolomieu collapse during the March–May 2007 distal eruption and associated ground displacements. (A) On March 30th, a vertical magma injection propagated from the shallow magma reservoir below Dolomieu crater (B) fast lateral magma injection leading to the early stage of the summit deflation; (C) underground collapse of the reservoir roof rock; (D) surface collapse. The collapse acted as a piston on the reservoir and increased the emission rate in surface (Gauss Laborde Réunion coordinates).

The fast draining of the shallow reservoir had repercussions on the fractured rock column above the reservoir (Fig. 14B, C). Thus until April 5th the deflation source was not the magma reservoir itself, but the rock column that extended from 1150 m to 2300 m elevation (Figs. 10 and 14C). Several hypotheses can be advanced to explain the elongation of the pressure source: (1) a global contraction of the rock column by closing voids or small-scale cavities related by recurrent collapses since 2000 or (2) an upward migration of a same deflation source: from March 30th to April 5th, progressive upward stoping and migration of an underground cavity could have generated volume changes through the fractured rock column (Fig. 14C). Because of the small magnitude of displacements relative to the GPS background noise (error), we are unable to investigate the process on smaller time scale and to see in detail if an upward migration stoping occurred.

In the hypothesis of an upward migration stoping, the deep cavity was able to progress quickly to the surface because the rock column had already been weakened by intense brecciation and pre-existing faults and joints, similar to the mechanism proposed by Okubo and Martel (1998) and Walker (1999) for Hawaiian pit-craters. On April 5th at 14:28, an increase of inward displacements and eruptive tremor occurred until the surface collapse at 20:48. Numerical modelling suggests for this period a shallow deflated source located just below the surface at 2250 m of elevation (around 300 m depth) (Fig. 10).

#### 5.2.2. April 5th–6th: surface collapse

The first major collapse occurred on April 5th at 20:48 after 7 h of strong summit deflation, triggering a large 3.2 Md volcano-tectonic earthquake. This sudden collapse was followed by continuous cyclic subsidence until April 6th. Each cycle was characterized by a progressive inward deflation of the summit zone and ended by sudden

summit outward displacements linked with a collapse event (Figs. 2D and 3D). The short-lived outward displacements were caused by stress relaxation following each collapse event.

These successive cycles reveal that caldera formation did not result from a single event but from several collapses on April 5th and 6th increasing the depth of the Dolomieu crater by 340 m. Field observations on April 6th revealed that the collapse had affected first the northern part of the Dolomieu (Michon et al., 2007a). Two annular plateaus corresponding to the pre-existing floor of Dolomieu remained in the E and SW but collapsed on April 10th.

From April 5th to April 6th, the brecciated rock column subsided into the reservoir and acted as a piston that increased the internal pressure of the reservoir and thus the magma flux in the dyke feeding the eruptive fissure (Fig. 14D). The erupted lava flux has been estimated around  $200 \text{ m}^3 \text{ s}^{-1}$  on April 6th, against a mean of  $54 \text{ m}^3 \text{ s}^{-1}$  over the whole eruption (Staudacher et al., 2009-this issue).

#### 5.2.3. After April 6th: summit deflation

The majority of the Dolomieu crater collapse was rapid and occurred in only 24 h. However, the draining of the magma reservoir progressively enlarged the caldera with small landslides of the caldera walls until the end of the eruption. Following the short break on eruptive activity on April 10th, the eruptive tremor and the surface activity were lower, probably due to a decrease of the reservoir draining, generating a decrease of the summit deflation rate.

## 6. Conclusions

The study of ground displacements preceding and accompanying the April 2007 Dolomieu collapse allows us to constrain its origin and its dynamics. The main results can be summarized as follows:

- (1) Between 2000 and 2007, successive eruptions weakened and destabilized the host rock located above the shallow magma reservoir;
- (2) The fast draining of the shallow magma reservoir at the beginning of the March–April 2007 distal eruption, caused a gravity-driven piston-like downward displacement of its roof;
- (3) During the 5 days preceding the collapse, summit deflation was caused by volume change through the fractured rock column above the shallow magma chamber due to the closure of voids or small-scale cavities or the upward stopping and migration of an underground cavity;
- (4) During the 7 h before the onset of the collapse, the deflation source was located at ~300 m depth revealing the initiation of the collapse at very shallow depth;
- (5) On April 5th, at 20:48, the Dolomieu collapse initiated and consisted of many individual cycles over 24 h. Each cycle was characterized by a progressive inward deflation of the summit zone and ended by sudden summit outward displacements linked with a collapse event;
- (6) The subsidence of the rock column into the magma reservoir on April 5th–6th increased the eruptive flux;
- (7) After the end of the eruption, minor readjustments of the summit cone persisted for months with a slight summit deflation and small landslides of the caldera walls.

### Acknowledgements

We are grateful to Philippe Catherine, Philippe Kowalski and Frédéric Lauret for their help in implementing the GPS network, and to Patrice Boissier for his help in the automatic processing of GPS data. We thank William Chadwick, Laurent Michon and an anonymous reviewer for helpful advices and comments. This is IGP contribution number 2427.

### References

- Acocella, V., Tibaldi, A., 2007. Understanding caldera structure and development: an overview of analogue models compared to natural calderas. *Earth-Sci. Rev.* 85 (3–4), 125–160. doi:10.1016/j.earscirev.2007.08.004S.
- Bachèlery, P., 1981. Le Piton de La Fournaise (île de La Réunion). Etude volcanologique structurale. Thèse de spécialité Thesis, Université de Clermont Ferrand.
- Carter, A., van Wyk de Vries, B., Kelfoun, K., Bachèlery, P., Briole, P., 2007. Pits, rifts and slumps: the summit structure of Piton de La Fournaise. *Bull. Volcanol.* 69, 741–756. doi:10.1007/s00445-006-0103-4.
- Cayol, V., 1996. Analyse élastostatique tridimensionnelle du champ de déformations des édifices volcaniques par éléments frontières mixtes. doctorat Thesis, Université de Paris VII.
- Cayol, V., Cornet, F.H., 1997. 3D mixed boundary elements for elastostatic deformation field analysis. *Int. J. Rock Mech. Min. Sci.* 34 (2), 275–287.
- Cole, J.W., Milner, D.M., Spinks, K.D., 2005. Calderas and caldera structures: a review. *Earth Sci. Rev.* 69 (1–2), 1–26.
- De Natale, G., Pingue, F., 1993. Ground deformations in collapsed caldera structures. *J. Volcanol. Geotherm. Res.* 57, 19–38.
- Fukushima, Y., Cayol, V., Durand, P., 2005. Finding realistic dike models from interferometric synthetic aperture radar data: the February 2000 eruption at Piton de La Fournaise. *J. Geophys. Res.* 110 (B03206). doi:10.1029/2004JB003268.
- Geshi, N., Shimano, T., Chiba, T., Nakada, S., 2002. Caldera collapse during the 2000 eruption of Miyakejima Volcano, Japan. *Bull. Volcanol.* 64 (DOI 10.1007/s00445-001-0184-z), 55–68.
- Hirn, A., Lépine, J.-C., Sapin, M., Delorme, H., 1991. Episodes of pit-crater collapse documented by seismology at Piton de la Fournaise. *J. Volcanol. Geotherm. Res.* 47, 89–104.
- Lénat, J.-F., Bachèlery, P., Bonneville, A., Hirn, A., 1989. The beginning of the 1985–1987 eruptive cycle at Piton de La Fournaise (La Réunion); new insights in the magmatic and volcano-tectonic systems. *J. Volcanol. Geotherm. Res.* 36, 209–232.
- Letourneur, L., Peltier, A., Staudacher, T., Gudmundsson, A., 2008. The effects of rock heterogeneities on dyke paths and asymmetric ground deformation: the example of Piton de La Fournaise (Réunion Island). *J. Volcanol. Geotherm. Res.* 173 (3–4), 289–302.
- Longpré, M.A., Staudacher, T., Stix, J., 2007. The November 2002 eruption at Piton de La Fournaise volcano, La Réunion Island: ground deformation, seismicity, and pit crater collapse. *Bull. Volcanol.* 69, 511–525.
- Macdonald, G.A., Abbott, A.T., Peterson, F.L., 1970. *Volcanoes in the Sea: The Geology of Hawaii*. Univ Hawaii Press.
- Michon, L., Staudacher, T., Ferrazzini, V., Bachèlery, P., Marti, J., 2007a. April 2007 collapse of Piton de La Fournaise: a new example of caldera formation. *Geophys. Res. Lett.* 34 (L21301) doi:1029/2007GL031248.
- Michon, L., Saint-Ange, F., Bachèlery, P., Villeneuve, N., Staudacher, T., 2007b. Role of the structural inheritance of the oceanic lithosphere in the magmato-tectonic evolution of Piton de la Fournaise volcano (La Réunion Island). *J. Geophys. Res.* 112, (B04205). doi:10.1029/2006JB004598.
- Michon, L., Villeneuve, N., Catry, T., Merle, O., 2009. How summit calderas collapse on basaltic volcanoes: New insights from the April 2007 caldera collapse of Piton de la Fournaise volcano. *J. Volcanol. Geotherm. Res.* 184, 138–151 (this issue).
- Munro, D.C., Rowland, S.K., 1996. Caldera morphology in the western Galapagos and implications for volcano eruptive behaviour and mechanisms of caldera formation. *J. Volcanol. Geotherm. Res.* 72, 85–100.
- Okubo, C.H., Martel, S.J., 1998. Pit crater formation on Kilauea volcano. *Hawaii. J. Volcanol. Geotherm. Res.* 86, 1–18.
- Peltier, A., 2007. Suivi, Modélisation et Evolution des processus d'injections magmatiques au Piton de La Fournaise. Université de La Réunion. 365 pp.
- Peltier, A., et al., 2008. Cyclic magma storages and transfers at Piton de La Fournaise volcano (La Réunion hotspot) inferred from deformation and geochemical data. *EPSL* 270 (3–4), 180–188.
- Roche, O., van Wyk de Vries, B., Druitt, T.H., 2001. Sub-surface structures and collapse mechanisms of summit pit craters. *J. Volcanol. Geotherm. Res.* 105, 1–18.
- Sambridge, M., 1999a. Geophysical inversion with a neighbourhood algorithm — i. Searching a parameter space. *Geophys. J. Int.* 138, 479–494.
- Sambridge, M., 1999b. Geophysical inversion with a neighbourhood algorithm — ii. Appraising the ensemble. *Geophys. J. Int.* 138, 727–746.
- Simkin, T., Howard, K.A., 1970. Caldera collapse in the Galapagos Islands, 1968. *Science* 169, 429–437.
- Staudacher, T., Ferrazzini, V., Peltier, A., Kowalski, P., Boissier, P., Catherine, P., Lauret, F., Massin, F., 2009. The April 2007 eruption and the Dolomieu crater collapse, two major events at Piton de la Fournaise (La Réunion Island, Indian Ocean). *J. Volcanol. Geotherm. Res.* 184, 126–137 (this issue).
- Urai, M., Geshi, N., Staudacher, T., 2007. Size and volume evaluation of the caldera collapse on Piton de la Fournaise volcano during the April 2007 eruption using ASTER stereo imagery. *Geophys. Res. Lett.* 34 (L22318). doi:10.1029/2007GL031551.
- Walker, G.P.L., 1999. Volcanic rift zones and their intrusion swarms. *J. Volcanol. Geotherm. Res.* 94, 21–34.